Pergamon

Solid State Communications, Vol. 90, No. 8, pp. 523–526, 1994
Elsevier Science Ltd
Printed in Great Britain
0038-1098/94 $7.00 + .00

0038-1098(94)E0109-O

# IDENTIFICATION OF Xe INTERFACE STATES IN THE Xe(1 1 1)/Pt(1 1 1) SYSTEM BY SPIN-RESOLVED PHOTOELECTRON SPECTROSCOPY

B. Kessler*, N. Müller, B. Schmiedeskamp and U. Heinzmann

Universität Bielefeld, Fakultät für Physik, 33501 Bielefeld, Germany and Fritz-Haber-Institut der MPG, 14195 Berlin, Germany

(*Received* 22 *November* 1993; *accepted for publication* 26 *January* 1994 *by P.H. Dederichs*)

New electronic states at the Xe(1 1 1)/Pt(1 1 1) interface are identified to be Xe-3*p*-derived states by spin resolved photoelectron spectroscopy using circularly polarized radiation from the BESSY 6.5 m NIM beamline. Their initial energies lie above the valence band maximum of bulk Xe. The final state energy and spin polarization is determined by bulk Xe conduction band states.

SPIN-RESOLVED photoemission data from Xe(1 1 1) crystals grown on Pt(1 1 1) are presented, and cannot be interpreted in terms of the Xe bulk bandstructure. Emission from states within the fundamental band gap of bulk Xe is found. Although photon energies below the threshold of 9.8 eV for direct photoemission from a Xe crystal [1] are used, the results are accounted for in terms of interface states without resorting to an explanation based on excitonic states [2–4].

The experiments have been carried out at the 6.5 m NIM-beamline at BESSY [5]. The circularly-polarized light ranging in energy from 9 to 14.5 eV is incident normal to the (1 1 1)-face of the Xe crystal. The Xe crystals consist of 10–15 monolayers epitaxially grown on a Pt(1 1 1) substrate at approximately 40 K. They have proven to be sufficiently thick to result in photoemission spectra as a 3D-crystal without carrying the disadvantage of charging effects during the photoemission experiment [6, 7].

Electrons emitted inside an acceptance cone of 4.5° around the surface normal are energy analyzed and their spin-polarization component $P$ along the direction of light incidence is measured by a Mott detector. The total energy resolution (consisting of the monochromator resolution and the electron spectrometer resolution) is about 150 meV (for further details of the apparatus see [8] and [9]). Positive and negative $P$ means preferential directions of the electron spin parallel and antiparallel to the photon spin, respectively. The spin dependent results are expressed by partial electron intensities $I_+$ and $I_-$, depending on $P$ and on the total electron intensity $I_0$ by: $I_+ = 1/2I_0(1 + P)$, $I_- = 1/2I_0(1 - P)$.

Figure 1 shows spin-resolved photoelectron energy distribution curves from Xe(1 1 1) on Pt(1 1 1). The initial energy is determined by a procedure described in detail in [6], where a symmetry-resolved band mapping of Xe in the Λ-direction has been performed using the same adsorbate system. It refers to the valence-band maximum (VBM) of the Xe crystal, such that positive values represent energies in the fundamental gap region. The photon energy is varied between 9 and 10 eV. At $h\nu = 9$ eV very low intensities with $I_-$ dominating are observed on the low-energy edge of the spectrum. When going from $h\nu = 9.4$ to 9.6 eV a peak $A_1$ in the $I_-$-intensity grows at an initial energy of about 0.8 eV. At lower initial energy, a peak $B_1$ in the $I_+$-channel appears and seems to be completely developed at $h\nu = 9.6$ eV. Its initial energy corresponds to about 0.4 eV. A further peak $A_2$ appears in the $I_-$-channel at $h\nu = 9.6$ eV. Due to the vacuum edge, the initial energy of this peak cannot be determined unambiguously from the spectra. At a photon energy of 10 eV (which is 0.2 eV above the photoemission threshold for a Xe crystal) the direct photoemission from valence-band states of the Xe crystal with initial energies below 0 eV appears and dominates the spectrum.

* Present address: Forschungszentrum Jülich (IFF), 52425 Jülich, Germany.

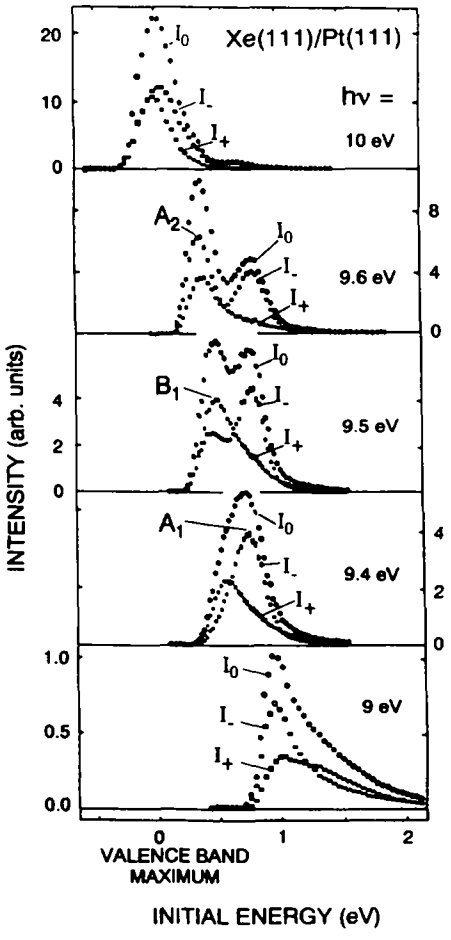


Fig. 1. Spin-resolved photoelectron spectra from Xe(1 1 1)/Pt(1 1 1) at various photon energies. Given are the total electron intensity $I_0$, the partial intensities $I_+$ and $I_-$. See the text for the peak assignments. The height of the $I_+/I_-$-symbols represents the total error including the uncertainties of light polarization and of the Mott-detector polarization sensitivity. The energy scale refers to the VBM of the Xe-crystal (positive values are in the fundamental gap). The spectra are normalized to equal light flux. The uncertainty of the photon energy due to the monochromator calibration is about 0.1 eV.

The peaks with initial energies above 0 eV in Fig. 1 cannot be interpreted by direct transitions between bands of an ideal 3D Xe crystal because their initial energy is located within the fundamental gap. Emission via excitonic states can also be excluded, as the initial-state energy does not vary with photon energy [3, 4]. As photoemission from one and two Xe-layers on Pd(1 1 1) shows a corresponding peak $A_1$ located 0.7 eV above VBM and also a peak $B_1$ separated from $A_1$ by −0.6 eV [7], we interpret peak $A_1$ and peak $B_1$ to originate from states of the first Xe layer (interface layer) in contact with the Pt-substrate derived from the ($p_{3/2}$, $|m_j| = 3/2$)- and from the ($p_{3/2}$, $|m_j| = 1/2$)-hole state of the Xe ion, respectively. The separation of the peaks $A_1$ and $B_1$ depends on the Xe–Xe interaction and therefore varies depending on the structure [8, 10]. The preferential spin directions found in the peaks $A_1$ and $B_1$ are identical in both experiments. Therefore, we assume the existence of transitions from the occupied states of the first Xe layer into unoccupied states which are totally symmetric. Peak $A_2$ is interpreted to originate from the ($p_{3/2}$, $|m_j| = 3/2$) derived stated of the second Xe layer shifted against $A_1$ primarily due to a smaller final-state screening of the ionic Xe hole state by the metallic substrate [11, 12]. An observation of further peaks at lower initial energies is not possible because of the high intensity of the direct photoemission from Xe(1 1 1) above 9.8 eV.

Figure 2 illustrates the model described above. Two additional $p_{3/2}$-derived flat bands $A_1$, $B_1$ are drawn into the bandstructure of a Xe crystal along Λ [6, 13]. They are expected to have no dispersion along

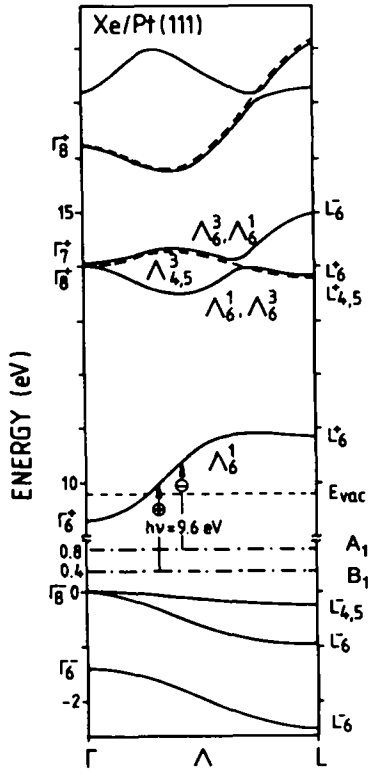


Fig. 2. Bandstructure of bulk Xe along the Λ-direction [6, 13] with additional flat interface bands $A_1$, $B_1$ from the first Xe layer in contact with the Pt(1 1 1)-substrate. The energy scale refers to the VBM of the Xe crystal. Arrows show typical transitions for $h\nu = 9.6$ eV. The signs +/− denote the preferential spin direction of the transition. Unoccupied $\Lambda^3_{4,5}$-bands are shown as dashed lines.

Λ (the lack of dispersion can, however, not explicitly be proven experimentally because the region in $k$-space sampled is too small when the photon energy is varied by the small amount of 0.2 eV) because the interface layer is a 2D-system normal to Λ. Their location within the fundamental gap of the Xe crystal is caused by a final-state screening by the metallic substrate lowering the binding energy against the binding energy of the $p_{3/2}$-derived bulk bands [11, 12].

The final states for the observed photoemission from the interface layer are composed of three parts: an unoccupied bulk Xe state from a band along Λ, a vacuum state matched to this state and a Xe-substrate interface state. The interface state will have a symmetry derived from the bulk state. The measurements for the system of two Xe-layers on Pd(1 1 1) [7] confirm this statement. The bulk-derived part of the final state restricts the energy of the final state to a sharp $E(k)$ (like an energy filter). Therefore, there is no smearing out of the energetic position due to the broken 3D-symmetry at the interface or at the surface, as was found in [7].

With photon energies between 9 and 10.2 eV photoemission from the occupied interface layer band $A_1$ via final states determined by the first unoccupied Xe bulk band is possible. This range of photon energies corresponds to energies between the vacuum level at 9.8 eV and the upper edge of this band at about 11 eV. This is reflected in Fig. 1 by the onset of the peak $A_1$ at $h\nu = 9$ eV and the significant reduction of its intensity at $h\nu = 10$ eV. The preferential spin directions found in the data given in Fig. 1 for the peak $A_1$ and for the peak $B_1$ are consistent with the $\Lambda^3_{4,5}$, $\Lambda^3_6$ symmetries of the bands $A_1$ and $B_1$, respectively, and with the $\Lambda^1_6$ symmetry of the first unoccupied bulk band participating in the emission (relativistic dipole selection rules, see [14]).

The model is tested further by increasing the photon energy. In the bulk bandstructure of Xe along Λ, two strongly hybridized $\Lambda^1_6$, $\Lambda^3_6$-bands and one $\Lambda^3_{4,5}$-band follow the first unoccupied band after a second gap of about 2.5 eV at energies from 13.5 to 15 eV (see Fig. 2). Figure 3 shows results for a photon energy of 13.5 eV. The structures below the VBM have been identified in an earlier paper [6]. A weak maximum in the $I_+$ channel occurs at about 0.8 eV. This maximum is assigned to be peak $A_1$ which has changed its preferential spin direction compared with Fig. 1. The reason for this change is evident by inspecting the bulk states in Fig. 2 with energies near $(0.8 + 13.5)$ eV $= 14.3$ eV. The upper $\Lambda^1_6$, $\Lambda^3_6$-hybridized band and the $\Lambda^3_{4,5}$-band are present at this energy. As the $\Lambda^{1,3}_6$-band here follows the $\Lambda^3_{4,5}$-band it mainly has $\Lambda^3_6$-character. Due to the relativistic dipole

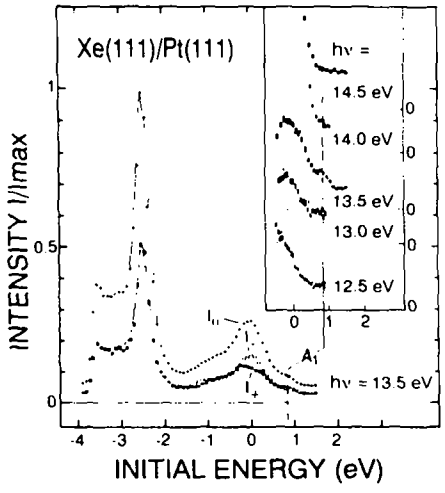


Fig. 3. Photoelectron spectrum from Xe(1 1 1)/Pt(1 1 1) at $h\nu = 13.5$ eV (see Fig. 1 for explanation of the energy scale and the errors). The inset gives a section of the spectra for initial energies around the energy of the $A_1$ interface state at varied photon energies. In the inset the intensity scale is expanded.

selection rules [14], starting from the interface band $A_1$ with $\Lambda^3_{4,5}$ symmetry, only transitions into the $\Lambda_6$-bands are possible. These transitions result in negative spin polarization if the $\Lambda^1_6$-part dominates the emission process and in positive spin polarization if the $\Lambda^3_6$-part dominates. Although the $\Lambda^3_6$-part cannot couple to vacuum states in normal emission, its amplitude is so strong that off-normal states within the 4.5°-acceptance cone of the energy analyzer dominate the emission spectrum [15].

The inset of Fig. 3 gives partial intensities for initial-state energies around the position of the $A_1$ interface band obtained with photon energies between $h\nu = 12.5$ and 14.5 eV. It shows the presence of the peak $A_1$ in the $I_+$-channel (filled rectangles) if the excitation just reaches the flat, high density of states region of the upper $\Lambda^1_6\Lambda^3_6$-band.

The intensity of peak $A_1$ in Fig. 3 is very low compared with that of Fig. 1. One reason may be that the kinetic energy of the electrons from peak $A_1$ is increased from less than 1 eV at $h\nu < 9.8$ eV to more than 4 eV at $h\nu = 13.5$ eV. This should cause a dramatic decrease in the mean free path of the electrons. Assuming a distance between neighbouring Xe atoms of 4.37 Å [16] the electrons which cross at least Xe layers must traverse more than 35 Å. In electron-phonon scattering spectroscopy also, the escape depth of electrons with kinetic energies below 1 eV is demonstrated to be extremely large compared to the one of electrons with somewhat higher kinetic energies [17].

Photoelectron spectroscopy data from Xe-doped

Ar and Ne matrices show comparable results for photoemission from states of the guest atoms through the host conduction band [18]. One important question for these experiments is the energy transfer between host excitonic states and guest atomic levels. In the present case, the host and the guest levels are built up by the same material. The guest levels are just marked by their contact to the substrate. The present explanation, however, does not resort to an interpretation in terms of excitonic states.

In summary, 2D-Xe states at the Xe(1 1 1)/Pt(1 1 1) interface grown on a Pt(1 1 1) substrate have been detected by spin-resolved photoemission. They show no dispersion along Λ. The interface states are located within the fundamental band gap of the bulk Xe crystal primarily because of the final state screening by the metallic substrate. Dipole selection rules connect the symmetry of the interface states to the symmetry of the bulk Xe crystal and determine the spin polarization of the emitted electrons. Only those electrons which fit into the unoccupied bands of Xe(1 1 1) can be observed, which means that the Xe crystal acts as an energy filter for the transmitted electrons.

*Acknowledgments* – Thanks go to Kevin Colbow for critical reading of the manuscript and to Anders Nilsson for fruitful discussions. Support by the Bundesministerium für Forschung und Technologie (grant No. 05 5PAXB I) is gratefully acknowledged.

## REFERENCES

1. N. Schwenter, F.-J. Himpsel, V. Saile, M. Skibowski, W. Steinmann & E.E. Koch, *Phys. Rev. Lett.* **34,** 528 (1975).
2. *Electronic Excitations in Condensed Rare Gases* (Edited by N. Schwentner, E.E. Koch & J. Jortner), Springer, Heidelberg (1985).
3. G. Schönhense, *App. Phys.* **A41,** 39 (1986).
4. G. Schönhense, B. Kessler, N. Müller, B. Schmiedeskamp & U. Heinzmann, *Physica Scripta* **35,** 541 (1987).
5. F. Schäfers, W. Peatman, A. Eyers, Ch. Heckenkamp, G. Schönhense & U. Heinzmann, *Rev. Sci. Instrum.* **57,** 1032 (1986).
6. B. Kessler, A. Eyers, K. Horn, N. Müller, B. Schmiedeskamp, G. Schönhense & U. Heinzmann, *Phys. Rev. Lett.* **59,** 331 (1987).
7. B. Kessler, N. Müller, B. Schmiedeskamp, B. Vogt & U. Heinzmann, *Physica Scripta* **41,** 953 (1990).
8. A. Eyers, F. Schäfers, G. Schönhense, U. Heinzmann, H.P. Oepen, K. Hünlich, J. Kirschner & G. Borstel, *Phys. Rev. Lett.* **52,** 1559 (1984).
9. G. Schönhense, A. Eyers, U. Frieß, F. Schäfers & U. Heinzmann, *Phys. Rev. Lett.* **54,** 547 (1985).
10. B. Vogt, B. Kessler, N. Müller, G. Schönhense, B. Schmiedeskamp & U. Heinzmann, *Phys. Rev. Lett.* **67,** 1318 (1991).
11. G. Kaindl, T.-C. Chiang & T. Mandel, *Phys. Rev.* **B28,** 3612 (1983).
12. K. Jacobi, *Phys. Rev.* **B38,** 6291 (1988).
13. The bandstructure is based on calculations from J. Noffke, K. Hermann, M. Timmer & G. Borstel – for details see [6].
14. M. Wöhlecke & G. Borstel, in *Optical Orientation* (Edited by F. Meier & B.P. Zakharchenya), North Holland, Amsterdam (1984), p. 423.
15. S.V. Halilov, E. Tamura, H. Gollisch, R. Feder, B. Kessler, N. Müller & U. Heinzmann, *J. Phys.: Condensed Matter* **5,** 3851 (1993).
16. R.W.G. Wyckoff, in *Crystal Structures,* Vol. 2, 2nd edition, Interscience, New York (1964).
17. S.L. Molodtsov, C. Laubschat, G. Kaindl & V.K. Adamchuk, *Phys. Rev.* **B46,** 12802 (1992).
18. N. Schwentner & E.E. Koch, *Phys. Rev.* **B14,** 4687 (1976).